Congreso de Métodos Numéricos en Ingeniería
3-5 julio 2017, Valencia, España
© SEMNI, 2017

DC INTERNAL INDUCTANCE FOR A CONDUCTOR OF DIFFERENT RECTANGULAR CROSS SECTIONS COMPUTED WITH THE PARAMETRIC PROPER GENERALIZED DECOMPOSITION (PGD)

Manuel Pineda-Sanchez, Jordi Burriel-Valencia, Abel Sancarlos-González, Ruben Puche-Panadero, Juan Perez-Cruz

Universitat Politècnica de València
Camino de Vera s/n 46022 Valencia, Spain
e-mail: mpineda@die.upv.es, jorburva@ei.upv.es, absangon@upv.etsid.es, rupucpa@die.upv.es, juperez@die.upv.es, - Web page: http://www.upv.es

Keywords: PGD, DC Internal inductance, Parametric problems, Numerical methods, Inductance in rectangular cross section conductors.

Abstract *Rectangular conductors play an important role in industrial busbar systems, transformers, MEMs devices and planar transmission line structures. Unfortunately, no analytical expressions exist for obtaining the dc and the ac internal inductances or the ac resistance per-unit length of a linear conductor with a rectangular cross section, so that approximate expressions or numerically obtained charts must be used. This paper introduces a novel procedure for obtaining a "virtual chart", which gives the dc internal inductance of a rectangular conductor as a function of its thickness to width ratio, obtained in a single numerical simulation using the Proper Generalized Decomposition (PGD). The solution is obtained as a separated representation, which is, at the same time, very easy to store and very fast to operate with. The results obtained are compared with analytical solutions available in the technical literature. The proposed computation process can be easily extended to conductors of arbitrary shape, or to additional parametric dimensions as the frequency.*

1. INTRODUCTION

Rectangular conductors play an important role in planar transmission line structures, such as microstrip lines, coplanar strips, signal traces of printed circuit boards, and also in industrial busbars used in switchboards, distribution boards, or substation installations. The DC internal inductance of such a conductor is related to the magnetic energy stored within the conductor itself, and has a clear physical meaning, while the external inductance of a single conductor,

related to the magnetic energy stored in the field outside of the conductor, does not [1]. Unfortunately, no analytical expressions exist for obtaining the dc and the ac internal inductances or the ac resistance per-unit length of a linear conductor with a rectangular cross section, so that approximate expressions [1-3], or numerically obtained charts must be used. In this paper, a numerical method for obtaining the DC internal inductance of a rectangular conductor as a function of its thickness to width (t/w) ratio is presented, using the PGD ([4], [5], [9], [10]). The advantage of using a parametric formulation in this context is that the solutions for different rectangular conductors with a wide range of different t/w ratios are computed using a single simulation, and the solutions are obtained in a compact, separated representations form. The solution, expressed in this compact way, can be easily embedded in existing code for busbar analysis and design, instead of the usual look-up tables currently used. Besides, the proposed approach scales nicely with the number of parameters used in the simulation (frequency, etc.), which is not the case with high-dimensional look-up tables.

The procedure presented in this paper is not exclusive for rectangular conductors, which have been selected for illustrating the proposed approach due to its great industrial importance. On the contrary, the application of the procedure for other, non-rectangular cross-section shapes can be easily accomplished by replacing the separated representation of the rectangular cross-shape used in this paper with the desired one, without any further modification of the PGD algorithm presented here.

This paper is structured as follows. In Section 2, a brief reminder of the concept of the internal inductance of a conductor is presented, and a numerical approximation from [1] for the case of a rectangular conductor is given. Section 3 presents the PGD algorithm used to obtain the virtual chart of the dc inductance of this conductor for a wide range of t/w ratios, and the solution is compared with [1]. Section 4 presents the conclusions of this work.

2. INTERNAL INDUCTANCE FOR A CONDUCTOR

The internal inductance L_i per unit length of an infinitely long conductor of arbitrary shape is given by [1]

$$\frac{L_i}{l} = \frac{1}{I^2}\iint \vec{B}\cdot\vec{H}\,dS = \frac{1}{\mu_0 I^2}\iint \vec{B}\cdot\vec{B}\,dS = \frac{1}{\mu_0 I^2}\int_{\Omega_x}\int_{\Omega_y}\left(\mathrm{B_x}(x,y)^2 + \mathrm{B_y}(x,y)^2\right)dx\,dy, \quad (1)$$

where I is the current, the integral is carried out over the cross section of the conductor, and the conductor is assumed to be made of a non-magnetic material such as copper or aluminium, with magnetic permeability μ_0. Considering that the current has only a z-component (conductor parallel to the z axis, see Fig. 1), the magnetic vector potential (MVP) has also a single non-zero component, A_z, directed along the current. In this case, the components of the magnetic induction $\vec{B}$ in (1) can be expressed as:

$$\vec{B} = \nabla \mathrm{x} \vec{A} \rightarrow B_x = \frac{\partial A_z}{\partial y};\ B_y = -\frac{\partial A_z}{\partial x} \tag{2}$$

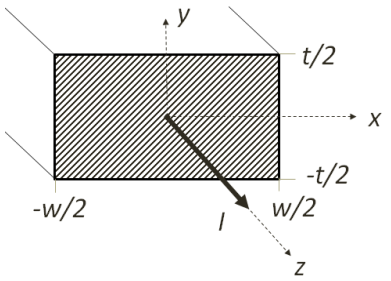

Figure 1. Conductor with rectangular cross-section, parallel to the *z*-axis.

The MVP generated by the conductor of Fig. 1 with a dc current density $J = I/(w \cdot t)$, where I is the total current carried by the conductor, can be obtained by considering that the conductor is made of elementary, infinitesimally thin sub-conductors, all of them with the same current density. A sub-conductor placed at the origin generates a MVP distribution given by

$$A_{z0}(x,y) = \frac{\mu_o I}{2\pi w t} \ln(x^2 + y^2) + C \tag{3}$$

where C is a constant value. The total MVP generated by the conductor is found by adding up the contribution of each sub-conductor, which results in the following integral expression

$$A_z(x,y) = \frac{\mu_o I}{2\pi w t} \int_{-\frac{t}{2}}^{\frac{t}{2}} \int_{-\frac{w}{2}}^{\frac{w}{2}} \ln\left[(x - x')^2 + (y - y')^2\right] dx' dy' + C \tag{4}$$

Applying (2) to (4) gives the components of the magnetic induction as

$$\begin{aligned} B_x(x,y) &= \frac{\mu_o I}{2\pi w t} \int_{-\frac{t}{2}}^{\frac{t}{2}} \int_{-\frac{w}{2}}^{\frac{w}{2}} \frac{(y - y')}{(x - x')^2 + (y - y')^2} dx' dy' \\ B_y(x,y) &= -\frac{\mu_o I}{2\pi w t} \int_{-\frac{t}{2}}^{\frac{t}{2}} \int_{-\frac{w}{2}}^{\frac{w}{2}} \frac{(x - x')}{(x - x')^2 + (y - y')^2} dx' dy' \end{aligned} \tag{5}$$

and, substituting (5) in (1), gives the expression of the internal dc inductance of the rectangular conductor as [1]

$$\frac{L_{idc}}{l} = \frac{\mu_0}{(2\pi wt)^2} \int_{-t/2}^{t/2} \int_{-w/2}^{w/2} [W_1^2 + W_2^2] dxdy \tag{6}$$

where W_1 and W_2 are given by

$$W_1 = \left(\frac{w+2x}{4}\right) \ln \left[\frac{\left(\frac{w}{2}+x\right)^2 + \left(\frac{t}{2}-y\right)^2}{\left(\frac{w}{2}+x\right)^2 + \left(\frac{t}{2}+y\right)^2}\right] + \left(\frac{w-2x}{4}\right) \ln \left[\frac{\left(\frac{w}{2}-x\right)^2 + \left(\frac{t}{2}-y\right)^2}{\left(\frac{w}{2}-x\right)^2 + \left(\frac{t}{2}+y\right)^2}\right] +$$
$$+ \left(\frac{t}{2}-y\right)\left[tan^{-1}\left(\frac{w-2x}{t-2y}\right) + tan^{-1}\left(\frac{w+2x}{t-2y}\right)\right] -$$
$$- \left(\frac{t}{2}+y\right)\left[tan^{-1}\left(\frac{w-2x}{t+2y}\right) + tan^{-1}\left(\frac{w+2x}{t+2y}\right)\right]$$

$$W_2 = \left(\frac{t+2y}{4}\right) \ln \left[\frac{\left(\frac{w}{2}-x\right)^2 + \left(\frac{t}{2}+y\right)^2}{\left(\frac{w}{2}+x\right)^2 + \left(\frac{t}{2}+y\right)^2}\right] + \left(\frac{t-2y}{4}\right) \ln \left[\frac{\left(\frac{w}{2}-x\right)^2 + \left(\frac{t}{2}-y\right)^2}{\left(\frac{w}{2}+x\right)^2 + \left(\frac{t}{2}-y\right)^2}\right] +$$
$$+ \left(\frac{w}{2}-x\right)\left[tan^{-1}\left(\frac{t-2y}{w-2x}\right) + tan^{-1}\left(\frac{t+2y}{w-2x}\right)\right] -$$
$$- \left(\frac{w}{2}+x\right)\left[tan^{-1}\left(\frac{t-2y}{w+2x}\right) + tan^{-1}\left(\frac{t+2y}{w+2x}\right)\right]$$

As [1] and [6] indicate, the integral (6) cannot be evaluated in closed form, because it results in poly-logarithms, which cannot be expressed in terms of elementary functions. So, the integral (6) must be computed numerically, for each value of the t/w ratio. Approximate formulae have been proposed in [1], [6] and [7] for the case of a small t/w ratio. The lack of closed solutions also arises in the cases of other conductor shapes, as in the case of conductors with elliptical or triangular cross-sections, as presented in [6].

3. PROPOSED APPROACH TO OBTAIN A PARAMETRIC SOLUTION OF THE DC INTERNAL INDUCTANCE FOR A RECTANGULAR CONDUCTOR USING THE PGD

The approach followed in this paper is different to the use of expressions to approximate the integral (6), as presented previously in the technical literature. Instead, the proposed method for obtaining the dc inductance of a rectangular conductor is based on solving the diffusion equation of the magnetic vector potential (MVP) of the conductor fed with a constant dc current,

$$\frac{\partial^2 A_z(x,y)}{\partial x^2} + \frac{\partial^2 A_z(x,y)}{\partial y^2} = -\mu_0 \cdot J_0\,(x,y) \quad with\ A_z|_{x=\infty} = A_z|_{y=\infty} = 0 \tag{7}$$

where J_0 is the density current through the conductor cross section. Traditionally, this equation must be solved numerically for each desired value of the t/w ratio of the conductor. Instead, using the PGD approach ([4], [5]), the t/w ratio can be considered as an additional dimension of the problem. That is, instead of computing the 2D MVP $A_z(x,y)$ in (7) as a function of the two spatial dimensions x, y, a 3D MVP $A_z(x,y,r)$ solution to (7) is sought, where r is an additional dimension used to represent the different values of the cross-sectional ratio of the conductor. The addition of the parameter r as a new dimension has a very low computational impact, and allows the construction of a virtual chart with the dc inductance of a rectangular conductor as a function of its t/w solving just a single problem in the extended domain Ω_x x Ω_y x Ω_r, that is:

$$\frac{\partial^2 A_z(x,y,r)}{\partial x^2} + \frac{\partial^2 A_z(x,y,r)}{\partial y^2} = -\mu_0 \cdot J_0\,(x,y,r) \quad with\ A_z|_{x=\infty} = A_z|_{y=\infty} = 0 \tag{8}$$

Using the PGD approach, the 3D MVP $A_z(x,y,r)$ in (8) is expressed as a sum of products of elementary one dimensional functions:

$$A_z(x,y,r) = \sum_{i=1}^{i=n} X_i(x) Y_i(y) R_i(r) \tag{9}$$

Each one of the n product terms that appear in (9) is termed a "mode", and, in the case of the MVP, they are automatically obtained following the PGD procedure, which is briefly presented in the next subsection, although an exhaustive explanation can be found in [4] and [5]. The value of n depends of the degree of accuracy used to represent the MVP, and is established using an error estimator in the PGD procedure.

The imposed current density in (8), $J_0\,(x,y,r)$, is represented also as a sum of products,

$$J_0(x,y,r) = \sum_{i=1}^{i=m} Jx_i(x) \cdot Jy_i(y) \cdot Jr_i(r) \tag{10}$$

In the context of the problem addressed in this paper, a particularly simple structure has been used for (10), which allows solving simultaneously (8) for a wide range of different

conductor's t/w ratios, as depicted graphically in Fig. 2:

- Each particular rectangular conductor i, among N_r different t/w ratios, can be represented with a single product $Jx_i(x) \cdot Jy_i(y)$ of the x and y components, each one having a 1 value under the projection of the conductor's shape on the respective axis, and 0 elsewere.

- The selection of a particular value of the t/w ratio is made through the dimension r in a straightforward way: the only non-zero element of the discrete component $Jr_i(r)$ is precisely $r = i$, and has the value of the current density imposed in the conductor, J. That is,

$$J_{ri}(r) = \begin{cases} J & r = i \\ 0 & r \neq i \end{cases} \qquad i = 0..N_r \tag{11}$$

This particular choice implies also that the number of modes of the imposed current density (10), m, is equal to the number of different t/w ratios that are to be computed, N_r, that is, $N_r = m$. The two first modes of the imposed current density are represented graphically in Fig. 2.

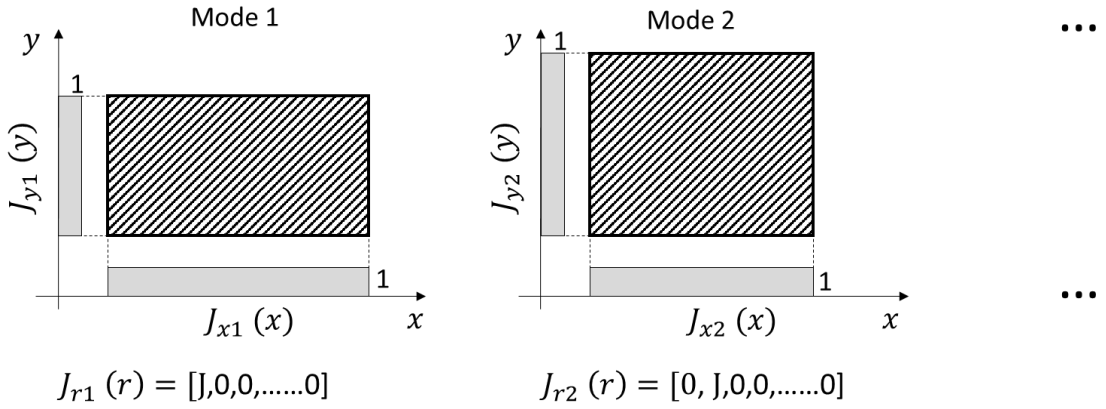

Figure 2. Modes used for representing a rectangular conductor with different t/w ratios using an additional r dimension.

To solve (8) numerically, the boundary condition at infinity in (8) is replaced by a boundary condition on a finite domain, $\Omega = \Omega_x \times \Omega_y = (-L, L) \times (-L, L)$, so that L is much greater than the dimensions of the conductor (in this work L is 100 times the width of the conductor). Using (9), (10) and (11), (8) can be expressed as:

$$\sum_{i=1}^{n}\left(\frac{\partial^2 X_i}{\partial x^2}Y_i\,R_i+X_i\frac{\partial^2 Y_i}{\partial y^2}\,R_i\right)\;=\;-\mu_0\sum_{j=1}^{m}Jx_j\cdot Jy_j\;\cdot Jr_j\quad with\;\;A_z|_{x=\pm L}=A_z|_{y=\pm L}=0 \tag{12}$$

The independent variables are no longer shown in (12) for simplicity. The functions X_i, Y_i and R_i can be computed numerically, using an iterative non-linear procedure. Supposing that the first (n-1) modes have been computed, the nth mode, unknown, is obtained via a Galerkin procedure applied to (12), as explained in full detail in [4] and [5]

$$\begin{gathered}A_z=\sum_{i=1}^{n}X_i\cdot Y_i\;\cdot R_i=\sum_{i=1}^{n-1}X_i\cdot Y_i\;\cdot R_i\;+X_n\cdot Y_n\cdot R_n\quad\Rightarrow\\ A_z^*=X_n^*\cdot Y_n\cdot R_n+\;X_n\cdot Y_n^*\cdot R_n+\;X_n\cdot Y_n\cdot R_n^*\end{gathered} \tag{13}$$

$$\int_{x=-L}^{x=L}\int_{y=-L}^{y=L}\int_{r=0}^{r=N_r}A_z^*\left[\sum_{i=1}^{n}\left(\frac{\partial^2 X_i}{\partial x^2}Y_i\,R_i+X_i\frac{\partial^2 Y_i}{\partial y^2}\,R_i\right)+\mu_o\sum_{j=1}^{m}Jx_j\cdot Jy_j\cdot Jr_j\right]dxdydr=0 \tag{14}$$

To find the mode n an iterative procedure is followed. Suppose that the functions Y_n and R_n are known at a given iteration, that is, $A_z^*=X_n^*\cdot Y_n\cdot R_n$. The substitution of (13) in (14) gives

$$\int_{x=-L}^{x=L}X_n^*\left(\begin{array}{l}\underbrace{\sum_{i=1}^{n}\left(\int_{y=-L}^{y=L}Y_n\frac{\partial^2 Y_i}{\partial y^2}dy\right)\left(\int_{r=0}^{r=N_r}R_nR_i dr\right)}_{\alpha_i}X_i+\underbrace{\sum_{i=1}^{n}\left(\int_{y=-L}^{y=L}Y_nY_i dy\right)\left(\int_{r=0}^{r=N_r}R_nR_i dr\right)}_{\beta_i}\frac{\partial^2 X_i}{\partial x^2}+\\ \underbrace{\mu_0\sum_{j=1}^{m}\left(\int_{y=-L}^{y=L}Y_nJy_j dy\right)\left(\int_{r=0}^{r=Nr}R_nJr_j dr\right)}_{\gamma_j}Jx_j\end{array}\right)dx=0 \tag{15}$$

This corresponds to the PDE

$$\sum_{i=1}^{n}\alpha_i\cdot X_i+\sum_{i=1}^{n}\beta_i\cdot\frac{\partial^2 X_i}{\partial x^2}+\sum_{j=1}^{m}\gamma_j\cdot\mu_0\cdot Jx_j=0 \tag{16}$$

And, moving all the known terms to the right-hand side (RHS), gives

$$\alpha_n \cdot X_n + \beta_n \cdot \frac{\partial^2 X_n}{\partial x^2} = -\sum_{i=1}^{n-1}\left(\alpha_i \cdot X_i + \beta_i \cdot \frac{\partial^2 X_i}{\partial x^2}\right) - \sum_{j=1}^{m}\left(\gamma_j \cdot \mu_0 \cdot Jx_j\right) \tag{17}$$

This equation is solved in the x domain with a simple 1D finite differences or a 1D FE method, giving the value of X_n in the present iteration. With this value, and assuming now X_n and R_n known, the computation of a new value of Y_n is performed as

$$\int_{y=-L}^{y=L} Y_n^* \left(\begin{array}{l} \sum_{i=1}^{n}\left(\int_{x=-L}^{x=L} X_n \frac{\partial^2 X_i}{\partial x^2} dx\right)\left(\int_{r=0}^{r=Nr} R_n R_i dr\right) X_i + \sum_{i=1}^{n}\left(\int_{x=-L}^{x=L} X_n X_i dx\right)\left(\int_{r=0}^{r=Nr} R_n R_i dr\right)\frac{\partial^2 Y_i}{\partial y^2} + \\ \qquad \alpha'_i \qquad\qquad\qquad\qquad\qquad\qquad \beta'_i \\ \mu_0 \sum_{j=1}^{m}\left(\int_{x=-L}^{x=L} X_n Jx_j dx\right)\left(\int_{r=0}^{r=Nr} R_n Jr_j dr\right) Jy_j \\ \qquad\qquad \gamma'_j \end{array} \right) dy = 0 \tag{18}$$

This corresponds to the PDE

$$\sum_{i=1}^{n} \alpha'_i \cdot Y_i + \sum_{i=1}^{n} \beta'_i \cdot \frac{\partial^2 Y_i}{\partial y^2} + \sum_{j=1}^{m} \gamma'_j \cdot \mu_0 \cdot Jy_j = 0 \tag{19}$$

and, moving all the known terms to the RHS, gives

$$\alpha'_n \cdot Y_n + \beta'_n \cdot \frac{\partial^2 Y_n}{\partial y^2} = -\sum_{i=1}^{n-1}\left(\alpha'_i \cdot Y_i + \beta'_i \cdot \frac{\partial^2 Y_i}{\partial y^2}\right) - \sum_{j=1}^{m}\left(\gamma'_j \cdot \mu_0 \cdot Jy_j\right) \tag{20}$$

This equation is solved in the y domain with a simple 1D finite differences or a 1D FE method, giving the value of Y_n. With this value, and assuming now X_n and Y_n known, the computation of a new value of R_n is performed as

$$\int_{r=0}^{r=Nr} R_n^* \left(\begin{array}{l} \sum_{i=1}^{n}\left(\int_{x=-L}^{x=L} X_n \frac{\partial^2 X_i}{\partial x^2} dx\right)\left(\int_{y=-L}^{y=L} Y_n Y_i dr\right) R_n + \sum_{i=1}^{n}\left(\int_{x=-L}^{x=L} X_n X_i dx\right)\left(\int_{y=-L}^{y=L} Y_n \frac{\partial^2 Y_i}{\partial y^2} dy\right) R_n + \\ \qquad \alpha''_i \qquad\qquad\qquad\qquad\qquad\qquad \beta''_i \\ \mu_0 \sum_{j=1}^{m}\left(\int_{x=-L}^{x=L} X_n Jx_j dx\right)\left(\int_{y=-L}^{y=L} Y_n Jy_j dy\right) Jr_j \\ \qquad\qquad \gamma''_j \end{array} \right) dr = 0 \tag{21}$$

This corresponds to the PDE

$$\sum_{i=1}^{n} \alpha"_i \cdot R_i + \sum_{i=1}^{n} \beta"_i \cdot R_i + \sum_{j=1}^{m} \gamma"_j \cdot \mu_0 \cdot Jr_j = 0 \tag{22}$$

and, moving all the known terms to the RHS, gives

$$(\alpha"_n + \beta"_n) \cdot R_n = -\sum_{i=1}^{n-1} \left((\alpha"_i + \beta"_i) \cdot R_i \right) - \sum_{j=1}^{m} \left(\gamma"_j \cdot \mu_0 \cdot Jr_j \right) \tag{23}$$

But (18) is just an algebraic equation, which gives directly the value of R_n as

$$R_n = \frac{-\sum_{i=1}^{n-1} \left((\alpha"_i + \beta"_i) \cdot R_i \right) - \sum_{j=1}^{m} \left(\gamma"_j \cdot \mu_0 \cdot Jr_j \right)}{(\alpha"_n + \beta"_n)} \tag{24}$$

finishing the present iteration. At every iteration the new values of X_n, Y_n and R_n are compared with the previous ones, and if the absolute value of their difference falls below a predefined threshold, the iterations are finished, and the solution is updated with the new values, corresponding to the n mode. This iterative process begins again for computing the next n+1 mode. When the absolute value of the new mode falls below a predefined threshold, the solution is considered valid and the process finishes. The whole process starts assuming that no mode is known, that is, n=0.

It is worth to mention that, contrary to the case of FEM, the addition of a new dimension r to obtain the MVP for a wide range of conductors with different t/w has a very low impact on the mathematical complexity of the PGD method, because it implies just solving a new algebraic equation, similar to (24). So, the PGD method encourages the use of additional, "parametric" dimensions which make possible to obtain the solutions of a given problem for a wide range of its characteristic parameters (such as the t/w ratio), with a cost comparable to the solution with just one particular value of these parameters.

Among the advantages of using the PGD for obtaining the internal inductance of the conductor with rectangular cross section, the following ones can be highlighted:

1. The 1D meshes used to obtain the 1D elementary functions $X_i(x)$ and $Y_i(y)$ can be very large and fine. If a mesh of N_x nodes is used for the x variable, and N_y nodes for the y variable, the number of nodes of the mesh is not $N_x \cdot N_y$, as expected when solving the 2D problem in (7), because only 1D PDE must be solved using (16) and (19). This feature allows for the use of uniform meshes that can be very large, to

properly establish the boundary conditions $A_z|_{x=\infty} = A_z|_{y=\infty} = 0$, and also very dense, to reach a high accuracy in the computation of the internal inductance, especially around the corners of the conductor cross section. The use of uniform meshes simplifies the solution of the problem, and in this paper the 1D PDEs have been solved using a simple finite difference method.

2. If a mesh of N_r nodes is used for the r variable, then N_r simulations of 2D dimensional problems (one for each t/w ratio) would be needed to calculate each solution of the MVP using traditional FEM methods. However, with the proposed approach, just one simulation is needed to obtain the MVP computed for the full range of t/w ratios corresponding to the N_r discrete values assigned to dimension r, which reduces the computer time required, compared with traditional numerical methods based on multidimensional meshes. Additionally, the decomposition achieved by the PGD allows storing all the solutions of the PDE more efficiently. The value of the MVP for a rectangular conductor with a given t/w ratio, corresponding to a value r_o, is given simply by

$$A_z = \sum_{i=1}^{i=n} X_i(x) Y_i(y) R_i(r = r_0) \tag{25}$$

3. To obtain the components of the magnetic induction (2) from the solution of the MVP in (8) it is not necessary to compute the full 2D representation of (9). Instead, the derivatives in (2) can be calculated directly using the separated 1D representation of (9), which allows to perform the integral (1) using simple 1D domains.

$$B_x = \frac{\partial A_z(x,y,r)}{\partial y} = \sum_{i=1}^{n} X_i(x) \cdot \frac{\partial Y_i(y)}{\partial x} \cdot R_i(r = r_0) \tag{26}$$

$$B_y = -\frac{\partial A_z(x,y,r)}{\partial x} = -\sum_{i=1}^{n} Y_i(x) \cdot \frac{\partial X_i(y)}{\partial x} \cdot R_i(r = r_0) \tag{27}$$

4. The method can be easily extended to conductors with any arbitrary cross-sections shapes. The only change to introduce is building the separated form of $J_0(x,y,r)$ (10) for the new geometries of the conductor.

4. RESULTS OBTAINED WITH THE PROPOSED APPROACH

The inductance of a conductor of rectangular cross-section has been obtained using the proposed method for different t/w ratios, and the results have been compared with the theoretical values given by (6), which has been integrated numerically. Figures 2, 3 and 4 show the results obtained with the PGD after solving (8). The 3D MVP of (9) has been

represented in these figures for three particular values of dimension r, those corresponding to t/w ratios equal to 1, 0.5 and 0.25.

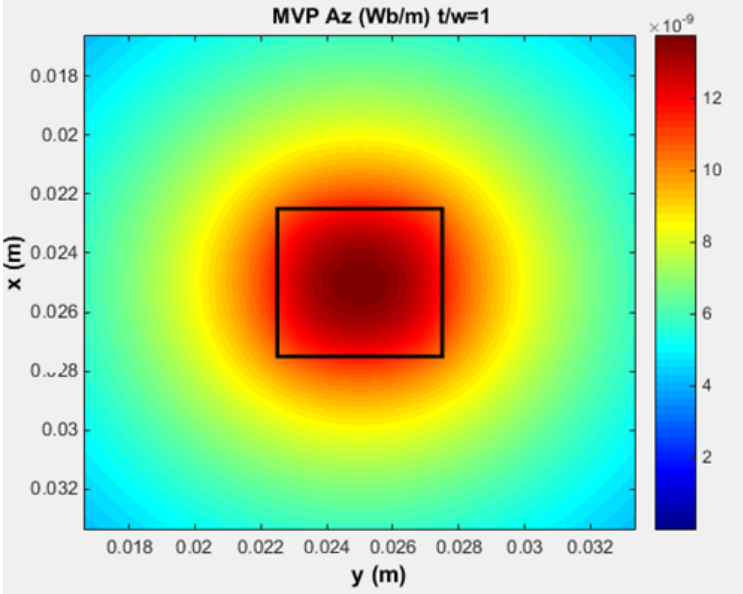

Figure 2. MVP generated by the conductor with rectangular cross-section with ratio t/w =1

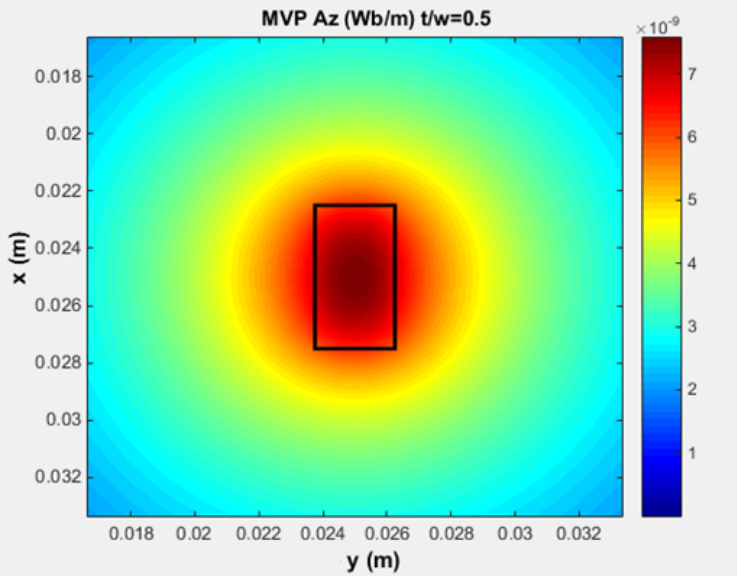

Figure 3. MVP generated by the conductor with rectangular cross-section with ratio t/w =0.5

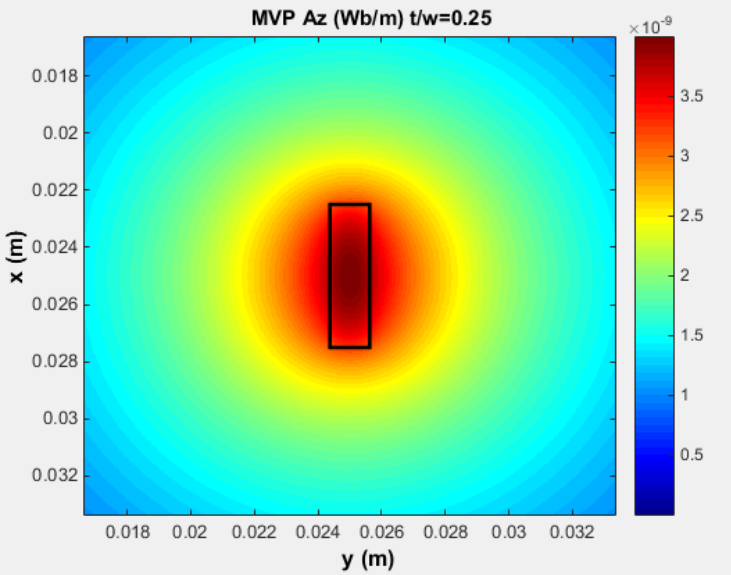

Figure 4. MVP generated by the conductor with rectangular cross-section with ratio t/w =0.25

The internal dc inductance of the conductor with rectangular cross section has ben obtained for different t/w ratios, and a plot of the results is presented in Fig. 5, along with the results obtained by numerical integration of (6).

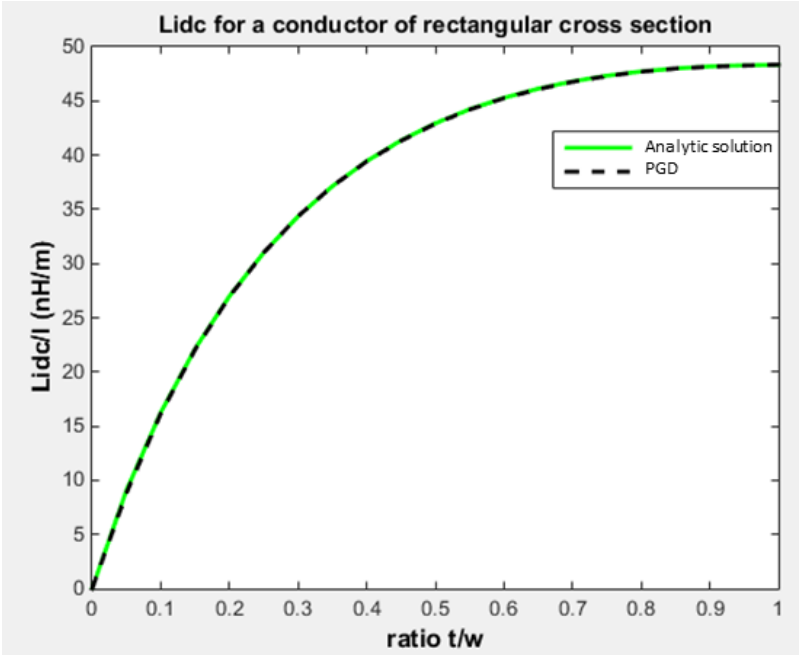

Figure 5. DC internal inductance Lidc of a conductor with a rectangular cross section, for different ratios t/w, computed by numerical integration of (6) and with the proposed approach.

5. CONCLUSIONS

In this paper, the PGD has been applied to compute the dc inductance of a conductor with rectangular cross section, as a function of its thickness to width t/w ratio. The use of a parametric formulation yields all the values for a wide range of t/w ratios, solving just one PDE in a multidimensional space (x, y, r), where a new dimension r accounts for all the possible values of the ratio t/w in a given range. The results have been found coincident with the numerical integration of the analytical formula available for this case, which validates the proposed approach. Besides, with the proposed method, the results obtained are available as a "virtual chart", which contains the solution for all of the values within the range of t/w ratios selected. The dc inductance of conductors with arbitrary shapes, other than the rectangular one, can be found easily with the proposed approach by just expressing this shape as a separated representation, easily computed using the SVD (Singular Value Decomposition). Following this approach, in a future work, the frequency of the current will be introduced also as an additional parametric dimension, which will generate a single 4D solution ($x, y, t/w$ ratio and frequency) that provides the internal inductance and the resistance of a rectangular conductor for any frequency and for any t/w ratio of the conductor.

ACKNOWLEDGEMENTS

This work was supported by the Spanish "Ministerio de Econom\ía y Competitividad" in the framework of the "Programa Estatal de Investigación, Desarrollo e Innovación Orientada a los Retos de la Sociedad" (project reference DPI2014-60881-R).

REFERENCES

[1] C. L. Holloway, S. Member, and E. F. Kuester, "*DC Internal Inductance for a Conductor of Rectangular Cross Section*" Electromagn. Compat. IEEE Trans., vol. 51, no. 2, pp. 338–344, 2009

[2] G. Antonini, A. Orlandi, S. Member, and C. R. Paul, "*Internal Impedance of Conductors of Rectangular Cross Section*" IEEE Trans. Microw. Theory Tech., vol. 47, no. 7, pp. 979–985, 1999.

[3] C. L. Holloway, E. F. Kuester, A. E. Ruehli, and G. Antonini, "*Partial and internal inductance: Two of Clayton R. Paul's many passions*," IEEE Trans. Electromagn. Compat., vol. 55, no. 4, pp. 600–613, 2013.

[4] F. Chinesta, A. Leygue, F. Bordeu, J. V Aguado, E. Cueto, D. Gonzalez, I. Alfaro, A. Ammar, and A. Huerta, "*PGD-Based Computational Vademecum for Efficient Design, Optimization and Control,*" Arch. Comput. Methods Eng., vol. 20, no. 1, pp. 31–59, 2013.

[5] F. Chinesta, P. Ladeveze, and E. Cueto, "*A Short Review on Model Order Reduction Based on Proper Generalized Decomposition,*" Arch. Comput. Methods Eng., vol. 18, no. 4, pp. 395–404, 2011.

[6] V. T. Morgan, "*The current distribution, resistance and internal inductance of linear*

power system conductors-a review of explicit equations," IEEE Trans. Power Deliv., vol. 28, no. 3, pp. 1252–1262, 2013.

[7] H. C. H. Chen and J. F. J. Fang, "*Modeling of impedance of rectangular cross-section conductors,*" IEEE 9th Top. Meet. Electr. Perform. Electron. Packag. (Cat. No.00TH8524), no. 83 1, pp. 159–162, 2000.

[8] E. Pruliere, F. Chinesta, and A. Ammar, "*On the deterministic solution of multidimensional parametric models using the Proper Generalized Decomposition,*" Math. Comput. Simulation, Elsevier, vol. 81, no. 4, pp. 791–810, 2012.

[9] González, D.; Aguado, J. V.; Cueto, E.; Abisset-Chavanne, E. & Chinesta, F., "*kPCA-Based Parametric Solutions Within the PGD Framework*", Archives of Computational Methods in Engineering, 2016, 1-18

[10] Heuzé, T.; Leygue, A. & Racineux, G., "*Parametric modeling of an electromagnetic compression device with the proper generalized decomposition*", International Journal of Material Forming, 2016, 9, 101-113